Hindawi Publishing Corporation
Advances in High Energy Physics
Volume 2013, Article ID 270792, 7 pages
http://dx.doi.org/10.1155/2013/270792

Research Article

Study of Neutrino Reactions for Low Values of Q^2

E. A. Paschos and Dario Schalla

Department of Physics, TU Dortmund, 44221 Dortmund, Germany

Correspondence should be addressed to Dario Schalla; dario.schalla@tu-dortmund.de

Received 24 June 2013; Revised 22 September 2013; Accepted 31 October 2013

Academic Editor: Srubabati Goswami

Low-energy neutrino interactions are calculated using results from PCAC and experimental data. The method is restricted to small values of Q^2 where it provides a benchmark for the axial form factor. Vector contributions were already determined using CVC. Comparisons with available data from recent experiments are satisfactory. The results indicate that three form factors $C_3^V(Q^2)$, $C_4^V(Q^2)$, and $C_5^A(Q^2)$ dominate in this kinematic region. The results are useful for investigations where the leptons scatter in the forward direction.

1. Introduction

Neutrino interactions at low and intermediate energies are attracting attention because they are used to interpret oscillation experiments and to discover new properties of neutrinos. Older calculations relied on PCAC and their estimates of the form factors [1, 2] are still used in Monte Carlo programs. In this paper, we specialize in a small kinematic region the small $Q^2 < 0.20\,\mathrm{GeV}^2$ because the various components of the cross-section can be correlated to other measurements through CVC and PCAC. We were motivated to adopt this approach by the presence of many form factors whose values at $Q^2 = 0$ and their Q^2 dependence are ambiguous. In a recent article [3], we proposed a program for constraining the number of amplitudes and we wish to present additional tests in order to confirm or disprove the method.

In this program, matrix elements of the vector current have been evaluated using the conserved vector current property by relating them to electroproduction. Matrix elements of the axial current are harder to estimate and we relate them through PCAC to pion reactions for $Q^2 < 0.20\,\mathrm{GeV}^2$. We adopt this principle because it has been tested in other processes where the absence of strong interaction singularities in a variable guarantees that the amplitudes vary smoothly with that variable. This method was used successfully in [3] and will also be extended to higher energies by another group [4] which will use coupled channels for estimating the hadronic reactions. Our main purpose here is to extend the program of [3] to many other reactions on free protons and neutrons, and to study the effects of the muon and electron masses in the final state. The limited range of Q^2 should not be worrisome because we are interested in establishing a few reliable couplings. Should many reactions to be measured for small Q^2 agree with the results in Figures 2, 3, and 4, then we will have a solid starting point.

In Section 2, we describe the method and show in Figure 1 the various components of the cross-section. The three contributions to the cross-section are shown explicitly and their magnitudes vary relative to each other with increasing neutrino energy. They provide correlations to be tested in experiments. Then we give the four possible reactions induced by neutrinos and antineutrinos and extend this method to neutral current reactions. The mass of the charged lepton in the final state has an effect on the small Q^2 region. We calculated the effects and show them in Figure 3.

In the previous article [3], we compared the results with the ANL, BNL, and the MiniBooNe data for the channel $\nu_\mu N \to \mu^- \pi^+$. In this paper, we extend the method to the other channel $\nu_\mu N \to \mu^- \pi^0 X'$, where N is the CH_2 molecule and X, X' are hadronic final states. For this experiment, we account for the rescattering effects in the ANP model based on an analytic solution of the transport equation in the nucleus. It includes absorption, the Pauli, and charge exchange effects. Agreement for the π^+ yield is good and for

the π^0 yield our curve is lower for $0.10 \le Q^2 \le 0.2\,\mathrm{GeV}^2$. The results are encouraging and point to several properties to be tested in future experiments. The purpose of our paper is to make available many cross-sections in this limited kinematic region, thus determining the dominant form factors.

Another approach uses an explicit model for the $WN \to \pi N'$ reaction including background terms from chiral symmetry [5]. The latest articles in this approach [5] prefer a larger value for $C_5^A(0)$ like 1.00 ± 0.11 close to the value of 1.2 that we use (see summary). Then, they fold the original model with medium effects and final state interactions (FSI). The model is applied over extensive kinematic regions by several groups [6–8]. Their results were discussed extensively in the last NUINT-2012 conference where the reader can find their conclusions [6–9]. In some kinematic regions of the MiniBooNE results, they underestimate the data with the missing pions being produced mainly in the forward direction. Their theory agrees better with data when FSI are not included. This paper treats also this forward region with results being closer to the data.

2. Description of the Method

The excitation of resonances by neutrinos involves vector and axial vector currents. For this reason, their hadronic matrix elements are expressed in terms of many form factors. For example, in the production of the Δ resonance the following form factors were introduced:

$$\begin{aligned}\mathscr{M} = \sqrt{\frac{3}{2}} G_F^2 \overline{\Psi}_\lambda\left(p'\right) \Bigg\{ & \left[C_3^V \frac{\gamma_\nu}{m_N} + C_4^V \frac{p'_\nu}{m_N^2} + C_5^V \frac{p_\nu}{m_N^2} \right] \gamma_5 F^{\lambda\nu} \\ & + \left[C_3^A \frac{\gamma_\nu}{m_N} + C_4^A \frac{p'_\nu}{m_N^2} \right] F^{\lambda\nu} \\ & + C_5^A j^\lambda + C_6^A \frac{q \cdot j q^\lambda}{m_N^2} \Bigg\} u(p),\end{aligned} \tag{1}$$

where $\Psi_\lambda(p')$ is the wave function of the delta, j^α is the leptonic matrix element $F^{\lambda\nu} = q^\lambda j^\nu - q^\nu j^\lambda$, and the Rarita-Schwinger spinor describes the $J = 3/2$ spin state.

As mentioned in the introduction, the vector form factors have been determined by electroproduction data [10] and their functional forms are given in equation (IV, 20) of [10]. Among the axial form factors, C_3^A was shown to be small by dispersion relation calculations [1]. In explicit calculations the contribution of $C_4^A(q^2)$ to the cross-section was shown to be small (see Figure 9 and equation (A2) in [11]). One reason is that in the kinematic regions we consider the lepton current j^ν is proportional to q^ν and the tensor $F^{\lambda\nu}$ vanishes.

The direct product of two leptonic currents can be expanded in terms of polarization four-vectors ϵ_μ^i with the coefficients being density matrix elements:

$$j_\mu \otimes j_\nu = \sum_{i,j} L_{ij} \epsilon_\mu^i \epsilon_\nu^j. \tag{2}$$

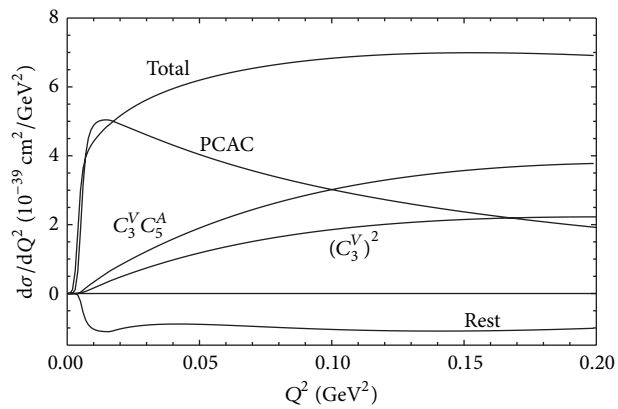

Figure 1: Anatomy of the various contributions to the cross-section at $E_\nu = 1$ GeV.

This was done in [12, 13] and the density matrix elements $L_{00}, \ldots$ were computed including the mass of the lepton [12]. In addition, the induced pseudoscalar term, which corresponds to C_6^A and contains the pion pole, combines with C_5^A [3] to produce the relation

$$C_5^A\left(Q^2\right) \overline{\psi_\lambda}\left(p'\right) q^\lambda u(p) = -f_\pi \langle \Delta \mid j_\pi \mid p \rangle, \tag{3}$$

where j_π is the pion source. The net effect is that the axial current alone produces the cross-section

$$\begin{aligned}\frac{d\sigma^{(A)}}{dQ^2 d\nu} = & \frac{G_F^2 |V_{ud}|^2}{8\pi^2} \frac{\nu f_\pi^2}{E_\nu^2 Q^2} \\ & \times \left[\widetilde{L}_{00} + 2\widetilde{L}_{l0} \frac{m_\pi^2}{Q^2 + m_\pi^2} + \widetilde{L}_{ll} \left(\frac{m_\pi^2}{Q^2 + m_\pi^2} \right)^2 \right] \\ & \times \sigma\left(\pi^+ p \longrightarrow \pi^+ p\right).\end{aligned} \tag{4}$$

The density matrix elements $\widetilde{L}_{00}$, $\widetilde{L}_{l0}$, and $\widetilde{L}_{ll}$ are given in [12, 13] and include the mass of the charged lepton in the final state. The cross-section $\sigma(\pi^+ p \to \pi^+ p)$ is the production of hadrons at the center of mass energy W for the reaction $\nu_\mu p \to \mu^- p \pi^+$ and is taken from [14]. In the present calculation, the $\pi^+ p \to \pi^+ p$ cross-sections are evaluated at W instead of ν, which was used in [3]. This modifies slightly the curves in Figure 1. A small improvement is the appearance of the additional terms proportional to $\widetilde{L}_{l0}$ and $\widetilde{L}_{ll}$. For each reaction, we use the appropriate experimental data. For instance, for the reaction $\nu_\mu n \to \mu^- p \pi_0$, we use the reaction $\sigma(\pi^+ n \to \pi^0 p) = \sigma(\pi^- p \to \pi^0 n)$ from [15], as we will discuss below. The fact that we use data means that the nonresonant background for the axial current is already included. For the vector and interference terms, we use the formalism of [3], where the vector form factors were determined for the $I = 3/2$ amplitudes. Precise electroproduction data established a small $I = 1/2$ nonresonant amplitude which we also include later by increasing the $C_3^V(0)$ form factor by 5% [16].

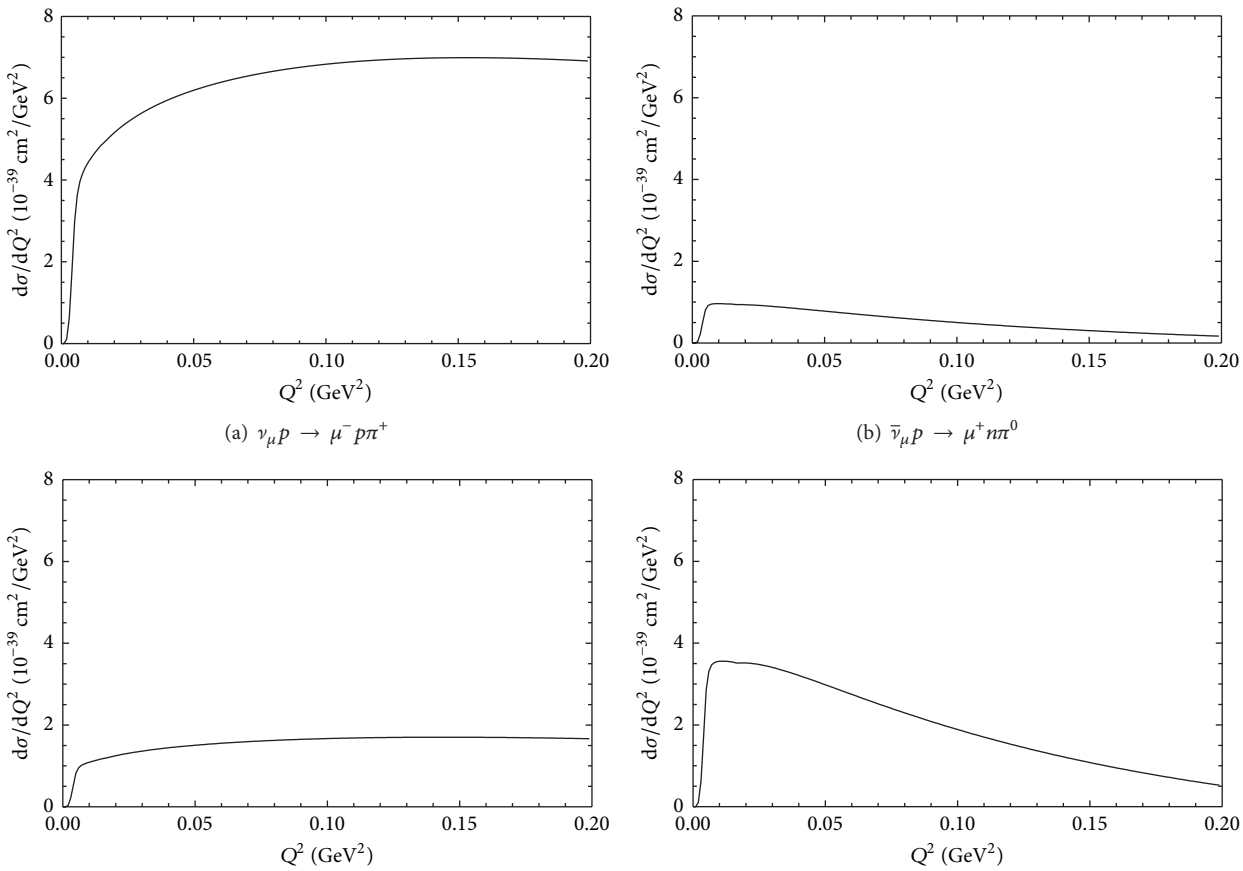

(a) $\nu_\mu p \to \mu^- p\pi^+$ (b) $\bar{\nu}_\mu p \to \mu^+ n\pi^0$

(c) $\nu_\mu n \to \mu^- p\pi^0$ (d) $\bar{\nu}_\mu n \to \mu^+ n\pi^-$

Figure 2: Charged current differential cross-sections for $E_\nu = 1$ GeV.

For the vector and interference terms, we use the formalism of [11] with the vector form factors from [10]. For the vector-axial interference $C_5^A C_3^V$, we use the form factor $C_5^A(Q^2)$ extracted through PCAC, and in addition $C_4^A = -(1/4)C_5^A$, suggested by PCAC, and the vector form factors just described. The sign of the interference term is constructive for neutrinos and destructive for antineutrinos. With these inputs we calculated the various contributions to the reaction $\nu_\mu p \to \mu^- p\pi^+$ shown in Figure 1. The curve denoted as "rest" indicates smaller contributions from additional form factors beyond C_3^V and C_5^A.

We repeated the computation for the reaction $\nu_\mu n \to \mu^- p\pi^0$ using data from [14]. We will use both cross-sections in the comparison with the MiniBooNE data [17, 18]. The results are shown in Figures 2(a) and 2(c). For antineutrino reactions, the sign of the $W_3(Q^2, \nu)$ changes. The antineutrino differential cross-sections are shown in Figures 2(b) and 2(d).

For experiments that use neutrino beams of the electron type, we replace the muon mass by the very small mass of the electron. The result for electron- and muon-neutrino cross-sections are shown in Figure 3 for various incident energies. For comparison, we include in the same figures the cross-sections for ν_μ beams. The muon mass turns the cross-sections to zero as $Q^2 \to 0$. The mass effect from the charged leptons is very visible. The turning of the ν_μ reaction toward zero occurs at smaller and smaller values of Q^2 as E_ν increases. For ν_e-induced reactions, the turning occurs at very small values of Q^2 which is not visible in the figure. It is however important to know the ν_e cross-sections since they enter experiments where ν_e's are regenerated through oscillations.

For neutral current reactions, there are more changes. The effective interaction is

$$\mathscr{H}_{\text{eff}} = \frac{G_F^2}{\sqrt{2}} \bar{\nu}\gamma^\mu (1-\gamma_5)\, \nu \left[x\mathscr{V}_\mu^3 + y\mathscr{A}_\mu^3 + \gamma\mathscr{V}_\mu^0 \right], \quad (5)$$

where $\mathscr{V}_\mu^3$ and $\mathscr{A}_\mu^3$ are the isovector and $\mathscr{V}_\mu^0$ the isoscalar hadronic currents. The parameters in the hadronic current are given in terms of the weak angle θ_W

$$x = 1 - 2\sin^2\theta_W, \qquad y = -1, \qquad \gamma = -\frac{2}{3}\sin^2\theta_W, \quad (6)$$

where $\sin^2\theta_W \approx 0.25$. The value of $y = -1$ gives a constructive $\mathscr{W}_3$ interference term (because of the structure of the lepton current $\bar{\nu}\gamma^\mu(1-\gamma_5)\nu$), making the neutrino reaction larger than the antineutrino.

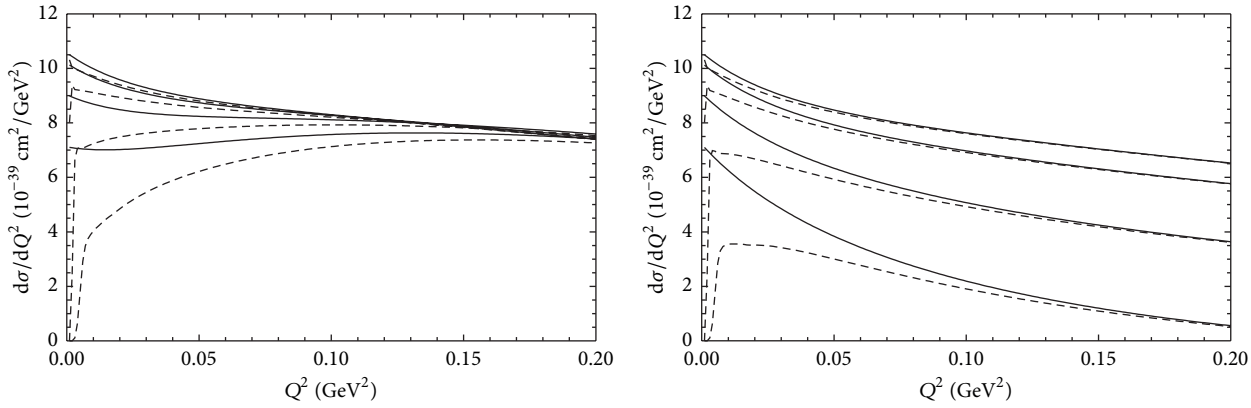

(a) $\nu_\ell p \to \ell^- p\pi^+$ (b) $\bar{\nu}_\ell n \to \ell^+ n\pi^-$

Figure 3: Comparison of muon and electron neutrino or antineutrino cross-sections for various energies $E_{\nu,\bar{\nu}} = 1, 2, 5, 10$ GeV (bottom to top). The solid line is for electron neutrinos or antineutrinos and the dashed one for muon neutrinos and antineutrinos, respectively.

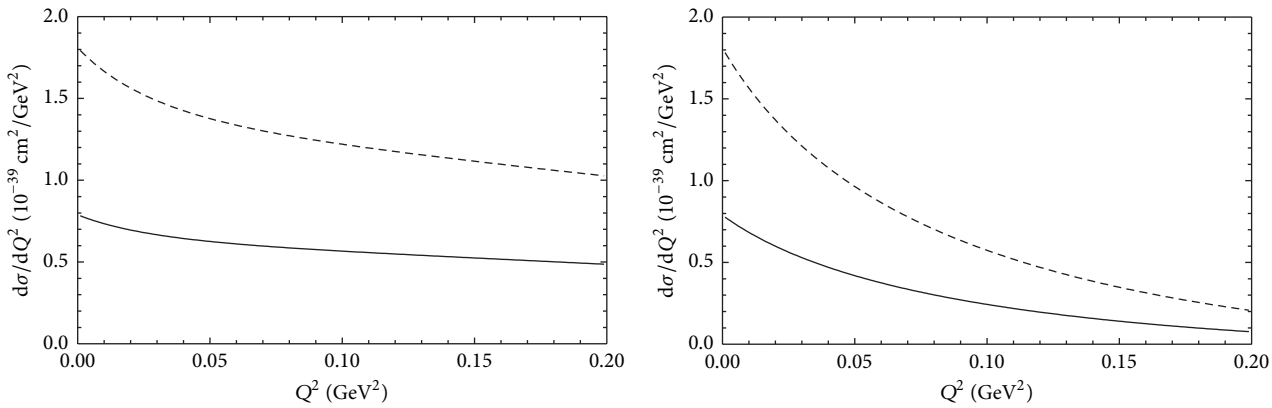

(a) $\nu_\mu p(n) \to \nu_\mu n\pi^+(p\pi^-)$ (solid), $\nu_\mu p(n) \to \nu_\mu p\pi^0(n\pi^0)$ (dashed) (b) $\bar{\nu}_\mu p(n) \to \bar{\nu}_\mu n\pi^+(p\pi^-)$ (solid), $\bar{\nu}_\mu p(n) \to \bar{\nu}_\mu p\pi^0(n\pi^0)$ (dashed)

Figure 4: Neutral current reactions at $E_\nu = 1$ GeV.

Beyond these parameters, there is an overall normalization factor in the amplitudes. In the charged current interaction appears the current

$$\mathscr{A}_\mu^1 + i\mathscr{A}_\mu^2 = \sqrt{2}\left(\frac{\mathscr{A}_\mu^1 + i\mathscr{A}_\mu^2}{\sqrt{2}}\right) = \sqrt{2}\mathscr{A}_\mu^+, \tag{7}$$

and for the neutral current $\mathscr{A}_\mu^3$. The The Clebsch-Gordan coefficients are valid for the triplet $(\mathscr{A}_\mu^+, \mathscr{A}_\mu^3, \mathscr{A}_\mu^-)$.

An additional property of neutral current reactions is

$$\begin{aligned} \sigma\left(\nu p \longrightarrow \nu\Delta^+\right) &= \sigma\left(\nu n \longrightarrow \nu\Delta^0\right) \\ \sigma\left(\bar{\nu} p \longrightarrow \bar{\nu}\Delta^+\right) &= \sigma\left(\bar{\nu} n \longrightarrow \bar{\nu}\Delta^0\right), \end{aligned} \tag{8}$$

which follows from isospin symmetry which for neutral current interactions is broken by the small term γV_μ^0. The calculated differential cross-sections for neutral currents are presented in Figure 4. The equalities in (8) were also confirmed by the results of an analytical calculation in Table 2 of [19]. The zero mass of the neutrino produces the finite values for the cross-sections at $Q^2 = 0$. This is also the exact point determined by PCAC where the neutrino and antineutrino cross-sections are equal. The results in Figures 2, 3, and 4 are some of the main results of this investigation because they give several cross-sections for reactions that have not been measured yet. It is our aim to restrict the presentation to small values of Q^2 where the input parameters are more reliable.

3. Comparison with Recent Experiments

In the previous section, we described the initial interactions on free protons and neutrons which we consider as benchmark. In the nucleus, the production and development of the resonance and of the decay products are influenced by the medium. The effects of the medium are included in a transport matrix [20–22] whose nature is determined by an absorption term and the interactions of the pions. The method was introduced by Fermi and includes the main features of multiple scatterings. The solutions are also analytic

which allows the reader to identify the origin of the effects. The multiple scattering of pions is governed by an inverse interaction length assumed to be the same for all pions, given by

$$\kappa = \rho(0)\,\sigma_{\text{tot}}(W), \tag{9}$$

$$\sigma_{\text{tot}}(W) = \sigma_{\text{abs}} + \frac{1}{3}\sigma_{\pi^+ p}(W)\left[h_+(W) + h_-(W)\right], \tag{10}$$

where $\rho(0)$ is the nuclear density at the center of the nucleus, $h_\pm(W)$ describes the forward- and backward-hemisphere projections of the Pauli blocking factor and σ_{abs} is the absorption cross-section given in equation (27) of [22]; it is a phenomenological function which contains several effects: the excitation of the nucleus, the propagation of the delta resonance before decay, and so forth.

Some authors compute the interaction of the delta with the medium as a self-energy correction [23] which shifts the mass and width of the resonance. Introducing a Breit-Wigner form for the resonance (with a corrected width $\Gamma + \delta\Gamma$) and taking its Fourier transform, it becomes evident that a shift in the width corresponds to a shift in the mean-free path:

$$\int_{-\infty}^{\infty} \frac{\mathrm{d}W\mathrm{e}^{iWt}}{(W-M)^2 + (\Gamma+\delta\Gamma)^2/4} = \frac{2\pi}{\Gamma}\mathrm{e}^{iMt}\mathrm{e}^{-((\Gamma+\delta\Gamma)/2)(z/v)}, \tag{11}$$

where $z = vt$ is the length of propagation and v is the velocity. This shift in the width of a resonance in momentum space corresponds to a shift in the inverse interaction length in configuration space. Thus, using σ_{abs} accounts for several effects.

During the propagation, scatterings take place as described by the pion-nucleon cross-sections at the center of mass energy of the delta resonance. The final yields of the pions ($\Sigma^f_{\pi^+}\ \Sigma^f_{\pi^0}\ \Sigma^f_{\pi^-}$) are obtained from the initial densities ($\Sigma^p_{\pi^+} + \Sigma^n_{\pi^+}, \Sigma^n_{\pi^0}, 0$) produced locally within the nucleus (see (18)–(20)). They are related through the transport equation

$$\begin{pmatrix} \Sigma^f_{\pi^+} \\ \Sigma^f_{\pi^0} \\ \Sigma^f_{\pi^-} \end{pmatrix} = M\left({}_6\mathrm{C}^{12}\right) = \begin{pmatrix} \Sigma^p_{\pi^+} + \Sigma^n_{\pi^+} \\ \Sigma^n_{\pi^0} \\ 0 \end{pmatrix}. \tag{12}$$

The transport matrix $M({}_6C^{12})$ has a simple form with an effective absorption factor $A(Q^2)$ and a charge exchange matrix. For the carbon target [24],

$$M\left({}_6C^{12}\right) = A\left(Q^2\right)\begin{pmatrix} 0.83 & 0.14 & 0.04 \\ 0.14 & 0.73 & 0.14 \\ 0.04 & 0.14 & 0.83 \end{pmatrix}, \tag{13}$$

with

$$A\left(Q^2 = 0.05\,\mathrm{GeV}^2\right) = 0.71, \tag{14}$$

$$A\left(Q^2 = 0.20\,\mathrm{GeV}^2\right) = 0.79, \tag{15}$$

$$A\left(Q^2 = 0.40\,\mathrm{GeV}^2\right) = 0.81. \tag{16}$$

The pion multiple-scattering is solved analytically as a stochastic problem [22]. The results of calculations confirm an old suggestion that charge-exchange corrections are substantial. They also follow a general principle: in a lepton-nucleus interaction the pions which have the same charge as the current are reduced. For pions with different charge than that of the exchanged current, the cross-section is enhanced.

We apply this formalism to the MiniBooNE results. The target in the experiment is the molecule CH_2, which we consider as the incoherent sum of C^{12} and two protons. This is justified since the two structures in the molecule are apart in comparison to the interatomic distance. The final yields of π^+ and π^0 are indicated by $\Sigma^f_{\pi^+}$ and $\Sigma^f_{\pi^0}$ and are obtained from

$$\Sigma^f_{\pi^+} = A\left(Q^2\right)\left\{0.83\left[\Sigma^p_{\pi^+} + \Sigma^n_{\pi^+}\right] + 0.14\Sigma^n_{\pi^0}\right\}6 + 2\Sigma^p_{\pi^+}, \tag{17}$$

$$\Sigma^f_{\pi^0} = A\left(Q^2\right)\left\{0.73\Sigma^n_{\pi^0} + 0.14\left[\Sigma^p_{\pi^+} + \Sigma^n_{\pi^+}\right]\right\}6. \tag{18}$$

The cross-sections within the brackets are defined as

$$\Sigma^p_{\pi^+} = \frac{\mathrm{d}\overline{\sigma}}{\mathrm{d}Q^2}\left(\nu_\mu p \longrightarrow \mu^- p\pi^+\right), \tag{19}$$

$$\Sigma^n_{\pi^+} = \frac{\mathrm{d}\overline{\sigma}}{\mathrm{d}Q^2}\left(\nu_\mu n \longrightarrow \mu^- n\pi^+\right), \tag{20}$$

$$\Sigma^n_{\pi^0} = \frac{\mathrm{d}\overline{\sigma}}{\mathrm{d}Q^2}\left(\nu_\mu n \longrightarrow \mu^- p\pi^0\right), \tag{21}$$

which we call the initial or primitive cross-sections. The bars over the cross-sections indicate averaging over the flux for $0.50\,\mathrm{GeV} \le E_\nu \le 2.00\,\mathrm{GeV}$ and are the cross-sections we computed for the spectrum of the MiniBooNE experiment using the result of Section 2.

The final yields for π^+ and π^0 are shown in Figure 5 where we plotted also the data from MiniBooNE. For the effective absorption factor $A(Q^2)$, we use the values from (14)–(16). The agreement of the π^+-yield with the data is good. For the π^0-yield, our curve is lower than the central value of the second bin by two standard deviations.

Looking into the composition of the yields, one finds the π^+ yield comes primarily from the direct production of π^+s with a small feeding from the π^0s. The π^0 yield, on the other hand, receives a substantial feeding from the primitive π^+. The contributions from the two terms, direct and feeding, are almost equal in this channel, as the reader can easily verify using the monoenergetic initial cross-sections in Figure 2 and the equations in this section. As we mentioned above, for the curves in Figure 5, we averaged over the neutrino spectrum. The contribution from charge exchange (feeding from the π^+ yield) compensates the reduction from $A(Q^2)$ and produces the solid curve in Figure 5. The fact that both theoretical curves in Figure 5 agree with the data for $Q^2 \le 0.10\,\mathrm{GeV}^2$ is in favor of PCAC. The values for $0.10\,\mathrm{GeV}^2 < Q^2 < 0.20\,\mathrm{GeV}^2$ being slightly smaller than the data calls attention to the absorption factor or to a background from higher resonances. This is a topic to be followed up by making comparisons in new experiments. The absorption of the pions in carbon may be smaller than the one introduced in (14) to (16).

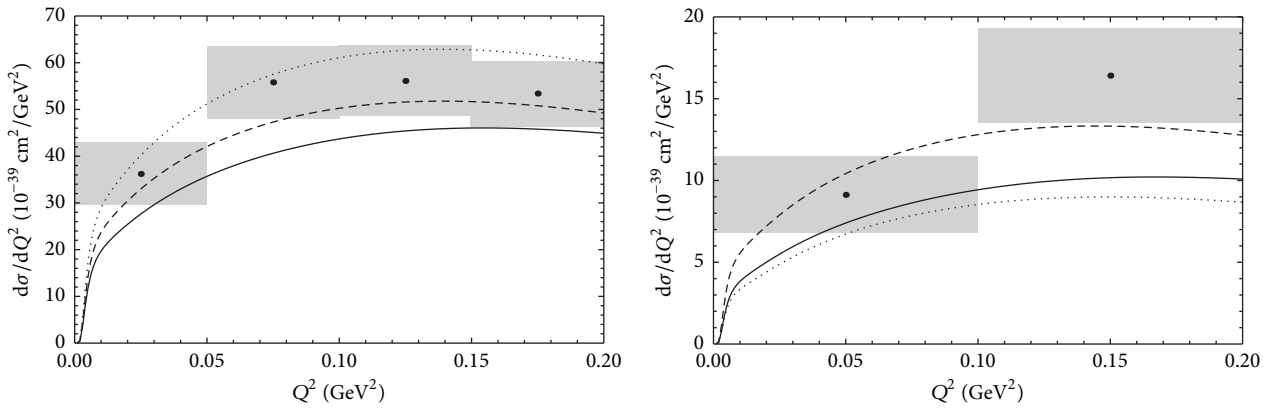

(a) π^+ yield (b) π^0 yield

Figure 5: Charged and neutral pion production for the MiniBooNE spectrum and comparison with experimental data. The dotted line is the cross-section without nuclear corrections, the dashed line with constant absorption $A = 0.9$, and the solid line with $A(Q^2)$ interpolated from (14) to (16). The curves with $A = 0.9$ give a better fit.

4. Summary and Conclusions

We presented a calculation for the production of pions by neutrinos in the small Q^2 region for energies (0.5–2.00 GeV). As we explain in the following paragraphs, the form factors we use are determined by PCAC, CVC, and experimental data. The results agree with the Argonne and Brookhaven data for the π^+ channel. We use the results for the initial cross-section to compute the yields of the MiniBooNE experiment which uses CH_2 as a target. This requires nuclear corrections for which we used the ANP model. The model was tested qualitatively for ratios of neutral-to-charged current reactions. The agreement for the $1\pi^+$ channel is good. For the $1\pi^0$ yield it is good for $Q^2 \leq 0.10\,\text{GeV}^2$, but our curve is lower than the data for $0.10 < Q^2 < 0.2\,\text{GeV}^2$. Comparisons in other nuclei will be useful to determine whatever improvements are needed for the effective absorption factor $A(Q^2)$, the charge exchange matrix, or both.

One of the uncertainties in neutrino reactions is the presence of many form factors whose Q^2 dependence is unknown and is determined by fitting data. We selected the kinematic region of small Q^2 where the lepton current j^μ is proportional to q^μ plus small corrections, so that the tensor $F^{\mu\nu}$ is small and the contribution of several form factors including $C_3^A(Q^2)$ and $C_4^A(Q^2)$ to the cross-section is suppressed. This is shown explicitly in Figure 9 of [11].

The status of the form factors is as follows. The magnetic dipole dominance was introduced in early articles of photo and electroproduction. Its implications for the form factors was worked out in the appendix of [25] and gave $C_4^V = -(m_N/W)C_3^V$ and $C_5^V(0) = 0$. An analysis of electroproduction amplitudes confirmed the magnetic dipole dominance (to within 5%) and determined their Q^2 dependence for $Q^3 \leq 3.0\,\text{GeV}^2$ (see Figure 4 in [10]).

There are also four axial form factors. PCAC gives the value $C_5^A(0) = 1.2$ and $C_4^A(Q^2) = -(1/4)C_5^A(Q^2)$. Newer values of $C_5^A(0)$ closer to 1.00 are still discussed and appear when a nonresonant background is introduced [26]. The remaining terms $C_3^A(Q^2)$ and $C_4^A(Q^2)$ disappear in the divergence of the axial current. They are like electric fields in classical electrodynamics whose divergence is zero. They must be detected in their interaction with the leptonic current. Our results in Figure 1 suggest a possibility. The proximity of the curves for $(C_3^V)^2$ and $C_3^V C_5^A$ in Figure 1, together with the fact that we know their relative contributions to the cross-section at other values of E_ν (see equations (A.1) and (A.3) in [11]), suggest that these two terms are canceled in antineutrino reactions. In this case cross-sections for antineutrinos, like the curves in Figures 2(b) and 2(d), are determined by PCAC and data alone. Any significant derivations from these curves as a function of Q^2 will indicate contributions from others form factors.

The cross-sections presented in this paper are also useful for determining the background to coherent scattering. We note that the background for antineutrinos is much smaller.

Acknowledgment

The authors wish to thank A. Higuera for useful discussions and for his help in preparing the paper.

References

[1] S. L. Adler, "Photo-, electro-, and weak single-pion production in the (3,3) resonance region," *Annals of Physics*, vol. 50, no. 2, pp. 189–311, 1986.

[2] D. Rein and L. M. Sehgal, "Neutrino-excitation of baryon resonances and single pion production," *Annals of Physics*, vol. 133, no. 1, pp. 79–153, 1981.

[3] E. A. Paschos and D. Schalla, "Neutrino production of hadrons at low energy and in the small Q^2 region," *Physical Review D*, vol. 84, no. 1, Article ID 013004, 7 pages, 2011.

[4] H. Kamano, S. X. Nakamura, T.-S. H. Lee, and T. Sato, "Neutrino-induced forward meson-production reactions in

nucleon resonance region," *Physical Review D*, vol. 86, no. 9, Article ID 097503, 5 pages, 2012.

[5] J. E. Amaro, E. Hernandez, J. Nieves, and M. Valcerde, "Theoretical study of neutrino-induced coherent pion production off nuclei at T2K and MiniBooNE energies," *Physical Review D*, vol. 79, no. 1, Article ID 013002, 18 pages, 2009.

[6] E. Hernandez, J. Nieves, and M. J. Vicente-Vacas, "One-pion production in neutrino-nucleus collisions," in *Proceedings of International Workshop on Neutrino-Nucleus Interactions in the Few-Gev Region (NUINT '12)*, Rio de Janeiro, Brazil, October 2012.

[7] O. Lalakulich and U. Mosel, "Pion production in the MiniBooNE experiment," *Physical Review C*, vol. 87, no. 1, Article ID 014602, 14 pages, 2013.

[8] J. T. Sobczyk and J. Zmuda, "Impact of nuclear effects on weak pion production at energies below 1 GeV," *Physical Review C*, vol. 87, no. 6, Article ID 065503, 16 pages, 2013.

[9] J. G. Morn, J. Nieves, and J. T. Sobczyk, "Recent developments in neutrino/antineutrino-nucleus interactions," *Advances in High Energy Physics*, vol. 2012, Article ID 934597, 35 pages, 2012.

[10] O. Lalakulich, E. A. Paschs, and G. Piranisvili, "Resonance production by neutrinos: the second resonance region," *Physical Review D*, vol. 74, no. 1, Article ID 014009, 14 pages, 2006.

[11] O. Lalakulich and E. A. Paschos, "Resonance production by neutrinos: $J = 3/2$ resonances," *Physical Review D*, vol. 71, no. 7, Article ID 074003, 10 pages, 2005.

[12] G. J. Gounaris, A. Kartavtsev, and E. A. Paschos, "Coherent pion production by neutrino scattering off nuclei," *Physical Review D*, vol. 74, no. 5, Article ID 054007, 9 pages, 2006.

[13] E. A. Paschos and D. Schalla, "Coherent pion production by neutrinos," *Physical Review D*, vol. 80, no. 3, Article ID 033005, 7 pages, 2009.

[14] J. Beringer, J.-F. Arguin, R. M. Barnett et al., "Review of particle physics," *Physical Review D*, vol. 86, no. 1, Article ID 010001, 1528 pages, 2012.

[15] M. E. Sadler, A. Kulbardis, V. Abaev et al., "Differential cross section of the charge-exchange reaction $\pi^- p \rightarrow \pi^0 n$ in the momentum range from 148 to 323 MeV/c," *Physical Review C*, vol. 69, no. 5, Article ID 055206, 10 pages, 2004.

[16] S. Galster, G. Hartwig, H. Klein et al., "Coincidence experiment on inelastic electron-proton scattering in the region of the $\Delta(1236)$ at q^2=−0.35 and −1.0(GeV/c)^2," *Physical Review D*, vol. 5, no. 3, pp. 519–527, 1972.

[17] C. E. Anderson, A. O. Bazarko, A. A. Aguilar-Arevalo et al., "Measurement of neutrino-induced charged-current charged pion production cross sections on mineral oil at $E_\nu \sim 1$ GeV," *Physical Review D*, vol. 83, no. 5, Article ID 052007, 26 pages, 2011.

[18] C. E. Anderson, A. O. Bazarko, A. A. Aguilar-Arevalo et al., "Measurement of ν_μ-induced charged-current neutral pion production cross sections on mineral oil at $E_\nu \epsilon 0.5$–2.0 GeV," *Physical Review D*, vol. 83, no. 5, Article ID 052009, 17 pages, 2011.

[19] E. Hernandez, J. Nieves, and M. Valverde, "Weak pion production off the nucleon," *Physical Review D*, vol. 76, no. 3, Article ID 033005, 22 pages, 2007.

[20] E. Fermi, "Sul moto dei neutroni nellesostanze idrogenate," *Ricerca Scientifica*, vol. 7, pp. 13–52, 1936.

[21] E. Amaldi, "The production and slowing down of neutrons," in *Handbuch der Physik*, S. Flugge, Ed., vol. 38, p. 557, Springer, Berlin, Germany, 1959.

[22] S. L. Adler, S. Nussinov, and E. A. Paschos, "Nuclear charge-exchange corrections to leptonic pion production in the (3, 3)-resonance region," *Physical Review D*, vol. 9, no. 7, pp. 2125–2143, 1974.

[23] E. Oset and L. L. Salcedo, "Delta self-energy in nuclear matter," *Nuclear Physics A*, vol. 468, no. 3-4, pp. 631–652, 1987.

[24] E. Paschos, I. Schienbein, and J.-Y. Yu, "Pion rescattering in nuclei," *Nuclear Physics B*, vol. 139, pp. 119–124, 2005.

[25] A. J. Dufner and Y. S. Tsai, "Phenomenological analysis of the γNN^* form factors," *Physical Review*, vol. 168, no. 5, pp. 1801–1809, 1968.

[26] E. Hernandez, J. Nieves, M. Valverde, and M. J. V. Vacas, "N-$\Delta(1232)$ axial form factors from weak pion production," *Physical Review D*, vol. 81, no. 8, Article ID 085046, 5 pages, 2010.